A model for rolling bearing life with surface and subsurface survival: Surface thermal effects

G.E. Morales-Espejel, A. Gabelli

A Model for Rolling Bearing Life with Surface and Subsurface Survival: Surface Thermal Effects

G.E. Morales-Espejel[1,2], A. Gabelli[1]

1) SKF Research and Technology Development
2) Université de Lyon, INSA-Lyon CNRS LaMCoS UMR5259 F69621, France

06-Aug-2020

Abstract

A previously developed model for bearing life calculation, based on high-cycle fatigue, including the separation of the surface and the subsurface survival of the rolling contact, is herewith further extended. It now includes the effects of frictional heating with a sharp temperature rise developed in the rolling contact. For this, a new surface damage integral, based on the creep mechanism, is included in the model. With this modification, the detrimental effect of high temperature developed in the rolling contact can now be accounted for. Sharp surface temperature rise during over-rolling are found in bearings operating at high speeds or under the combination of speeds, loads and unfavourable environmental temperatures. The present model introduces a threshold limit value of temperature above which the temperature in the rolling contact is deemed damaging for the steel microstructure and the tribological functionality of the rolling contact. The surface creep-damage model is first calibrated with endurance tests of bearings and then applied to study combinations of loads and speeds and the effect of the steel thermal conductivity on the life expectancy of the bearing. The ability of the present model to include damaging mechanisms, other than classical metal fatigue, increases the flexibility in bearing life predictions and allows to account for phenomena hitherto excluded from the estimation of the bearing fatigue life.

1. Introduction

Following current practices, the effect of the operating temperature in the estimation of the fatigue life of the bearing is accounted for by means of a lubrication quality factor (κ) as defined in ISO 281, [1]. An increase of the running temperature of the bearing corresponds to a reduction of the lubricant viscosity, hence a reduction of the lubrication quality which provides a penalisation of its expected fatigue life of the bearing. This standard approach is applicable for conventional operating conditions of the bearing which are defined in the standard ISO 281, [1] as: *"…conditions which may be assumed to prevail for a bearing which is properly mounted, conventionally loaded, not exposed to extreme temperature and not run at exceptionally low or high speed*."

Today a significant number of bearing applications are clearly outside the ISO 281 "*conventional*" area of operation. Indeed many relevant technical applications operate under very high speeds or combination of speed, load and environmental temperature that exceeds

the ISO and bearing catalogues recommended limits. The life performance estimation of such bearing applications is herewith addressed using a novel modelling approach based on the temperature-driven creep-damage accumulation of the raceway surface.

Tribological processes involving thermal cyclic damage can be related to e.g. frictional heating, metal softening by bulk heating and, in a way, also to electrical discharge damage due to current leakage in the rolling contact. These phenomena happen in combination with rolling contact fatigue and mild wear and, all of them, enter in competition to determine the life expectancy of the rolling contact. Under severe frictional heating during over-rolling, thermal loads tend to be dominant, reaching locally very high-temperature values. Above a threshold limit value, temperature-induced surface damage will determine the life of the contact either by local melting of the surface asperities (micro-smearing) or by low-cycle creep fatigue of the contact surface. On the other hand, metal softening by bulk heating refers to cases where the whole mechanical component is externally heated by the environment while is subjected to rolling contact fatigue. Considering that in this case, the surface is well lubricated, the bulk temperature effect is limited to moderate values and high cyclic (elastic) fatigue remains the dominant damage mechanism, although with material properties somehow reduced by the exposure to the thermal environment. Polonsky and Keer [2] have suggested that an increase in temperature in the steel can enhance localized carbon diffusion outflow affecting the fatigue behaviour of the steel.

All these thermal phenomena are not included in traditional bearing life models due to their complexity. Besides, most of the current bearing life models consider only subsurface rolling contact fatigue. In some cases, the rated life is also penalised with external life factors to account for other phenomena like poor lubrication, particle contamination [1] and other environmental conditions using a series of heuristic penalty factors independent from each other's and from the operating conditions of the bearing [3].

To improve this situation, recently, a new generalized modelling concept was pursued, [4]. In this new approach, surface and subsurface survival of the rolling contact are accounted with separate damage functions. This provides a clear advantage for the modelling capabilities of different failure modes point of view [4, 5, 6, 7, 8]. Reference [5] describes an special surface model to consider indentations on bearing raceways; reference [6] generalise the model of [4] to deal with gears; reference [7] tackles the case of hybrid bearings and reference [8] illustrates applications of this latest model. Up to now, this model includes only high-cycle fatigue as this is the most relevant degradation mechanism present in rolling bearings under conventional operating conditions. However, the model structure allows the consistent integration of other degradation processes occurring in the bearing, (either at the surface or in the subsurface of the rolling contact). This is very useful especially when it involves specific material degradation functions that depend on time, temperature or cycling stress.

Frictional heating of the contact and resulting sharp temperature rise in the rolling contact are significant aspects of the damage generation of certain thermally-induced failure modes of bearings, e.g. scuffing, smearing, electrical discharge damage and also the phenomenon known as seizure (which is the abrupt development of adhesive wear) which characterizes certain types of bearing failures occurring under very high speeds and loads [9]. As described in [9], the use of high speeds in bearings can produced kinematic starvation in the contacts (lack of replenishment of lubricant in the entrance due to the high number of rolling element passages on the raceway and little time for the lubricant to wet the surface again).

This effect combined with high contact loads can produce very high temperatures on the raceways surface.

Herewith, a temperature-driven, surface durability model based on the creep-damage accumulation of the raceway surface is presented. The model is incorporated into the existing generalized bearing life model, [4], comprising the surface and the subsurface survival of the rolling contact. The model is calibrated against experimentally obtained rolling bearing lives and is applied to study the effect of i) high speeds and loads, ii) different steel thermal conductivities. The current paper will deal with the effect of creep on the raceway surface. The bulk effect will not be covered in the current model. Although small modifications would be required to capture this effect.

It is found that under high-speed conditions, kinematic starvation dominates the performance of the bearing with direct effects on the frictional and thermal conditions of the rolling contact. This, in turn, sets limits to the life expectancy. While, under similar operating conditions, steel with higher thermal conductivity and the same fatigue strength, will result in increased fatigue performance. This is due to a lower equilibrium temperature of the rolling contact during bearing operation. Both model predictions were found in good agreement with the experimental observations.

2. Frictional Heating

The basic equations for a moving heat source are described in Carslaw and Jaeger [10]. A complete model for the calculation of surfaces in contact due to frictional heating is described in [11], therefore it will not be repeated here, only a brief summary is included.

A source heat is emitted at a certain geometrical origin at the rate of one heat unit per unit of time. Suppose that this heat is introduced in a moving semi-infinite homogeneous medium (with velocity u) parallel to the x axis. According to [10], the quasi-steady state surface temperature distribution is given by,

$$R(x,y) = \frac{1}{2\pi k_s \sqrt{x^2+y^2}} exp\left[-\frac{u}{2\chi}\left(\sqrt{x^2+y^2}-x\right)\right] \quad (1)$$

This equation can be extended for any source heat of shape $q(x,y)$. Thus, the quasi-steady state temperature distribution on the surface becomes,

$$T(x,y) = \int_A q(x',y')R(x-x',y-y')dA \quad (2)$$

With A being the surface area of the emitted heat source. Equation (2) also represents a space convolution between the functions $q(x,y)$ and $R(x-x',y-y')$, which alternatively can be solved with a simple element-to-element multiplication $(\cdot)$ of their FFT:

$$T(x,y) = IFFT\{FFT[q(x,y)] \cdot FFT[R(x,y)]\} \quad (3)$$

Now, the choice of the heat source shape R is important in the discretization process also. Here a mesh of $n_x \times n_y$ points is chosen with a rectangular constant heat source q_0 of dimensions Δ_x and Δ_y. Tian and Kennedy [12] propose the following equation to calculate the steady state temperature in any point (x, y, z) for a rectangular moving heat source:

$$R_r(x,y,z) = \int_{y-0.5\Delta y}^{y+0.5\Delta y} \int_{x-0.5\Delta x}^{x+0.5\Delta x} \frac{q_0}{2\pi k_s} exp\left\{\frac{u}{2\chi}[g-(x-x')]\right\} dx'dy' \quad (4)$$

Where $g = \sqrt{(x-x')^2 + (y-y')^2 + z^2}$, for the surface temperature $z = 0$. Since there is no simple analytical solution of equation (4) and the difficulties imposed by the singularity, thus the semi-analytical solution given by Bos and Moes [13] is followed.

In a lubricated contact, $q(x,y) = \mu p(x,y)$, where μ represents the average friction coefficient between lubricant and asperities in mixed-lubrication conditions. A methodology for the estimation of this parameter is given in [9] and followed here.

For two contacting bodies the generated heat in the interface will be split in different ways to the two bodies depending on the speed and thermal conductivity conditions, but the contacting temperatures on the two sides of the interface will be the same (assuming no thermal contact resistance). The temperature equations for the two surfaces are stablished and in the contacting points these temperatures will be equated, the heat distribution is found that fulfils this condition. The solution of this system is called the heat partition problem. Here the method given in [13] is followed.

3. Creep Damage Model

Collins [14] describes the competition of creep and elastic fatigue in structures with the following two possible models:

1. Linear Model:

$$D_f + D_{cr} \geq 1 \quad (5)$$

2. Quadratic Model:

$$(D_f)^2 + (D_{cr})^2 \geq 1 \quad (6)$$

Where D_f represents the damage accumulated by elastic fatigue and D_{cr} is the damage accumulated by isothermal creep.

Kachanov [15] and Rabotnov [16] introduce one of the first damage models related to creep in metals. Lemaitre and Desmorat [17] present a refined version of what they call the Kachanov law, describing the damage evolution in cyclic loading with creep, summarised in the following model (using the nomenclature of [17]):

$$\dot{D} = \left[\frac{\sigma}{A_D(1-D)}\right]^{r_D} \quad (7)$$

Where, $\dot{D} = dD/dt$, D is the damage parameter, $D < 1$ to avoid failure, A_D and r_D are material parameters depending upon the temperature and σ is the unidirectional stress applied during the time t. Rupture is reached when $D = 1$.

In those tribological problems where thermal effects are dominant, according to equations (5) or (6), the failure criterium can be simplified for creep to:

$$D_{cr} \geq 1 \tag{8}$$

Where equation (7) can be used. However, some simplifications are possible. Assuming that the thermal heating happens on a thin surface layer in the critical element with higher heating time so that permanent deformation can be ignored. The stress can be replaced by a function of temperature. Notice that in frictional heating, the surface temperature varies almost linearly with pressure, since the heat input is given by the surface shear stress and following equation (2) this gives a linear dependency. For electrical sparking problems, an extra temperature field (independent of stress) can be added. Therefore in general, the applied surface shear stress at every point on the surface can be approximated to $\sigma = BT$, where B is a constant and T is the local temperature depending also on the load. This can be substituted into equation (3) introducing $C = A_D/B$ and $r_D = m$, so:

$$\frac{dD}{dt} = \left[\frac{T}{C(1-D)}\right]^m \tag{9}$$

Now, it is also known that at relatively low temperatures (above ambient temperature) no damage is introduced by creep in steels used in tribological components, like gears and bearings. Therefore, one can introduce a minimum temperature below which the damage is basically zero, a sort of damage limit for temperature, T_u. In steels this temperature can be the microstructure transformation temperature limit (tempering). Depending on the bearing type, standard rolling bearings made from steels for through-hardening and surface hardening have recommended maximum operating temperature, which differs between 120 and 200^{0}C. The maximum operating temperature is directly related to the heat treatment process used in manufacturing components. For operating temperatures up to 250^{0}C; a special heat treatment (stabilization) can be applied. Most bearing manufacturers give recommended temperatures for their bearings, these values will set T_u. Thus, the temperature in equation (7) is replaced by:

$$T \rightarrow \ \Delta T = \langle T - T_u \rangle \tag{10}$$

Notice that in equation (10) a Macauley bracket notation has been introduced for which the term $\langle \ldots \rangle$ is set to zero if the quantity enclosed is negative. Therefore:

$$\frac{dD}{dt} = \left[\frac{\Delta T}{C(1-D)}\right]^m \tag{11}$$

The solution of equation (11) for D in Appendix A gives:

$$D = 1 - \left[1 - \frac{2a(m+1)(\Delta T)^m N}{C^m U}\right]^{\frac{1}{m+1}} \tag{12}$$

And the life time in terms of load cycles is:

$$N_{life} = \frac{C^m U}{(m+1)2a(\Delta T)^m} \tag{13}$$

Appendix B, shows different aspects of the behaviour of this model with simple examples, by varying the material parameters.

4. Bearing Life Model

Morales-Espejel et al. [4] introduced a bearing life model that accounts for the separation of surface and subsurface survival, the model was later adapted and also applied to gears [6]. The model as presented in [4] shows great flexibility to account different damage mechanisms as long as the material degradation functions are known. Previously only high-cycle fatigue was considered. However, equation (13) represents a new material degradation function for surface temperature damage, so there is no reason why this damage mechanism cannot be considered in the model of [4]. To incorporate this mechanism in the model one can consider the following.

The life of the surface via thermal degradation can be obtained from equation (13) for every point (x, y) on the bearing raceway surface:

$$uL(x,y) = \frac{C^m U}{(m+1)2a(\Delta T(x,y))^m} \tag{14}$$

Where u (as in [4]) is the number of stress cycles per revolution of the bearing. Now averaging the reciprocal of life along and across the raceway surface (A):

$$\frac{1}{uL} = \left[\frac{2a(m+1)}{C^m U}\right]\frac{1}{A}\int_A \langle T(x,y) - T_u\rangle^m dA \tag{15}$$

To obtain the material degradation function for this mechanism, one needs to compare equation (15) with the surface part of equation (15) of [5], the equation from the reference using the nomenclature of origin reads:

$$\frac{1}{L_s^e} = \frac{u^e \bar{B}}{\ln(S)} \int_A \langle \sigma(x,y) - \sigma_u\rangle^c dA \tag{16a}$$

Thus, for equation (15).

$$\frac{1}{L^e} = \frac{1}{\ln(S)}\left[\frac{2au(m+1)}{C^m UA}\right]^e \left[\int_A \langle T(x,y) - T_u\rangle^m dA\right]^e \tag{16b}$$

It is now convenient to simplify the exponent of the integral since $e \approx 1$, thus.

$$\frac{1}{L^e} = \frac{1}{\ln(S)}\left[\frac{2au(m+1)}{C^m UA}\right]^e \int_A \langle T(x,y) - T_u\rangle^m dA \tag{17}$$

Thus similar to equation (12) in [4], for every point on the raceway surface the material degradation function will be:

$$\hat{h}\int_A G_s(N)dA = \bar{C}^e(uL)^e\int_A \langle T-T_u\rangle^m dA \tag{18}$$

With e being the Weibull slope and with $A = 2al$. And $\bar{C} = \left[\frac{(m+1)}{C^m Ul}\right] = \left[\frac{(m+1)B^m}{A_D^m Ul}\right]$, with l being the length of the bearing raceway.

Finally equation (17) can be incorporated into equation (16) of [4] assuming equal Weibull slopes, and 90% reliability one obtains:

$$L_{10}^{-e} = \frac{u^e}{ln\left(\frac{1}{0.9}\right)}\left[\underbrace{\bar{A}\int_{V_v}\frac{\langle\sigma_v-\sigma_{u.v}\rangle^c}{z^h}dV_v}_{Subsurface} + \underbrace{\bar{B}\int_A\langle\sigma_s-\sigma_{u.s}\rangle^c dA}_{Surface} + \underbrace{\sum_{i=1}^{N}\bar{C}^e\left[\int_A\langle T-T_u\rangle^m dA\right]_i}_{Frictional\ Heating}\right] \tag{19}$$

This final equation includes in its last term a summation of thermal integrals because often more than one contact in a bearing is loaded. The equation can now be used to estimate the life of a rolling bearings including frictional heating and will be solved in the next section. The reader should notice that creep effects have only been incorporated in the surface (third integrals) in a independent fashion from fatigue. In a more general model the two mechanisms interact both in the surface and in the subsurface, this is indeed a matter of further investigations. However, equation (19) is limited to surface heating effects. High bulk temperatures will affect also the fatigue performance of the bearing, modifying the endurance constants $\bar{A}$ and $\bar{B}$ in the first and second integrals. In the present model these constants have been kept unchanged to their values corresponding to a temperature below T_u.

4.1. Competition of Mechanisms

The generalized bearing life model presented in [4, 5] introduces a surface damage ratio as,

$$R_I = \frac{\underbrace{\bar{B}\int_A\langle\sigma_s-\sigma_{u.s}\rangle^c dA}_{Surface}}{\underbrace{\bar{A}\int_{V_v}\frac{\langle\sigma_v-\sigma_{u.v}\rangle^c}{z^h}dV_v}_{Subsurface} + \underbrace{\bar{B}\int_A\langle\sigma_s-\sigma_{u.s}\rangle^c dA}_{Surface}} \tag{20}$$

This ratio represents the relative weight that the surface damage has in relation to the total damage. For $R_I = 1$ all the damage is taken by the surface and for $R_I = 0$ no damage is taken by the surface. For equation (19) similarly a "thermal" surface damage ratio can be defined as:

$$R_T = \frac{\underbrace{\sum_{i=1}^{N} \bar{C}^e \left[\int_A \langle T - T_u \rangle^m dA\right]_i}_{Frictional\ Heating}}{\underbrace{\bar{A} \int_{V_v} \frac{\langle \sigma_v - \sigma_{u.v} \rangle^c}{Z^h} dV_v}_{Subsurface} + \underbrace{\bar{B} \int_A \langle \sigma_s - \sigma_{u.s} \rangle^c dA}_{Surface} + \underbrace{\sum_{i=1}^{N} \bar{C}^e \left[\int_A \langle T - T_u \rangle^m dA\right]_i}_{Frictional\ Heating}} \tag{21}$$

Therefore when $R_T = 1$ all the damage is taken by the surface due to thermal effects and for $R_T = 0$ no damage is taken by the surface from thermal effects.

5. Results

5.1. Endurance Tests

Consider two full-bearing endurance tests, one lubricated with grease 1 (blue) and the other with grease 2 (red). See the Weibull curves resulting from the tests in Figure 1. Clearly longer life is found for the bearings running with grease 2.

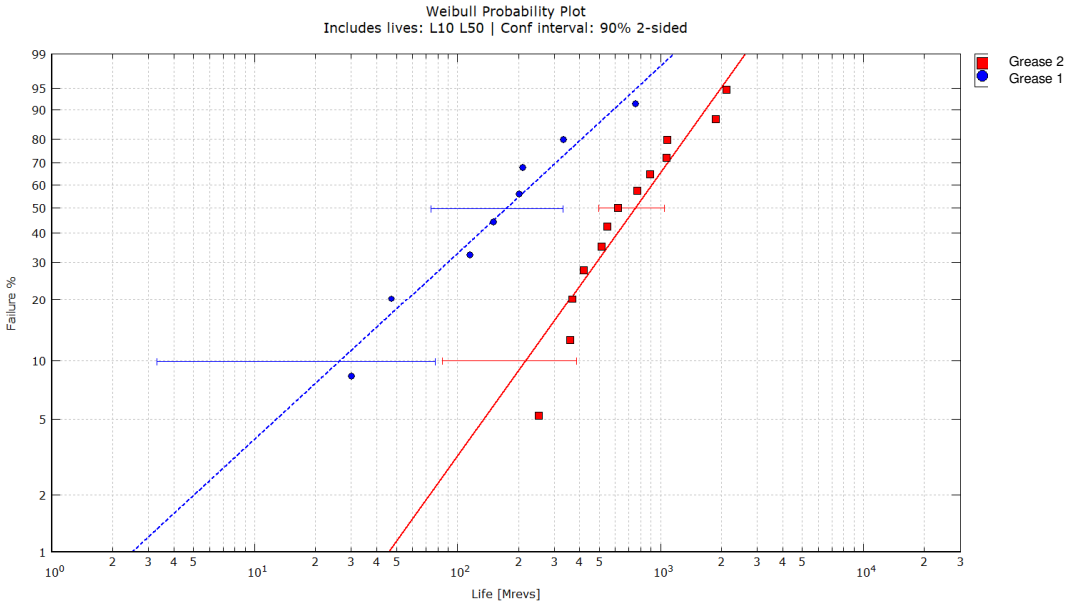

Figure 1. *Weibull curves for two endurance tests, one with grease 1 and the other with grease 2.*

The greases have similar base oil viscosities and similar thickener but they might have differences in temperature behaviour, grease life, additives and oil release behaviour (bleeding), the main features of the used greases are described in Table 1.

Table 1. *Greases used in the endurance tests of Figure 1.*

Grease	Thickener	Base Oil	Viscosity at 40^{0}C	Viscosity at 100^{0}C
Grease 1	di-urea	ester oil	95.1 cSt	12.1 cSt
Grease 2	di-urea	ether oil	81.6 cSt	10.8 cSt

The operating conditions and bearing designation are described in Table 2. In fact this is an extended test of one of the bearings described in [9]. The endurance tests are carried out at high temperature (160^0C) to simulate an electrical motor application. The tests were executed in test rigs SKF type 2 like the ones described in [18]. Pictures of typical failed and non-failed bearings are shown in Figure 2.

Table 2. *Summary of parameters of the endurance tests of Figure 1.*

Bearing designation	Nominal κ	T_{bulk} [^{0}C]	Lubricant	Material	Radial Load [N]	Static p_h, inner ring, [GPa]	nd_m
6202	0.63	160	Grease 1,2	52100	1300	3.0	450000

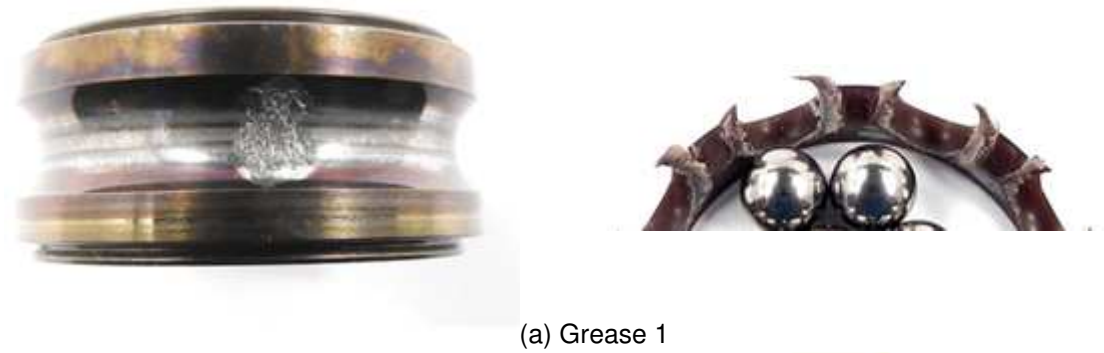

(a) Grease 1

(b) Grease 2

Figure 2. (a) *Photographs of typical failures in the endurance tests (grease 1), indicating inner ring spalling and surface discoloration and cage (glass-fibre reinforced polyamide) overheating due to high temperatures generated on the raceways. (b) shows a non-failed bearing showing nearly zero overheating running with grease 2.*

In order to model the effect on the bearing life of these two different greases, two approaches can be followed; i) to calculate the system (grease-bearing) life, since potentially

grease 1 has shorter life in these operating conditions the system life will be shorter in this case; ii) to reflect the visible thermal damage of the bearing in the model that calculates the bearing life, grease 1 produces higher thermal damage in the bearing and will produce shorter bearing life. In this paper the second approach is chosen.

5.2. Surface Temperature Calculations

In order to assess all the terms of equation (19) the third integral requires the calculation of the contact temperatures on the raceways due to frictional heating. Already in [9] a procedure to estimate the friction coefficient is given. Where also the modelling of kinematic starvation is included, particularly important in high speeds. However, for this case (relatively low velocity) the results of Table 4 and 5 from [9] show that "*theoretically*" kinematic starvation has no importance (grease 1) since the nominal lubrication quality parameter (κ) has the same value as the effective value ($\kappa = 0.63$) and the estimated average friction coefficient is $\mu = 0.051$. The thermal and mechanical properties for this bearing made of hardened ASTM 52100 steel are summarised in Table 3.

Table 3. *Summary of bearing material properties used.*

Hardened Steel (ASTM 52100)	**Value**	**Units**
Young modulus, E	206x10^9	[Pa]
Poisson ratio, ν	0.3	[-]
Thermal conductivity, k_s	23	[W/(mK)]
Specific heat, c_p	473	[J/(kg K)]
Density, ρ	7900	[kg/m^3]
Hardened High-Strength Stainless Bearing Steel	**Value**	**Units**
Young modulus, E	206x10^9	[Pa]
Poisson ratio, ν	0.3	[-]
Thermal conductivity, k_s	14	[W/(mK)]
Specific heat, c_p	490	[J/(kg K)]
Density, ρ	7900	[kg/m^3]

Finally, the sliding speed and contact pressure distribution in the inner and outer ring contacts are calculated, under the endurance test conditions, using a rolling bearing calculation software and Figure 3 summarises the results.

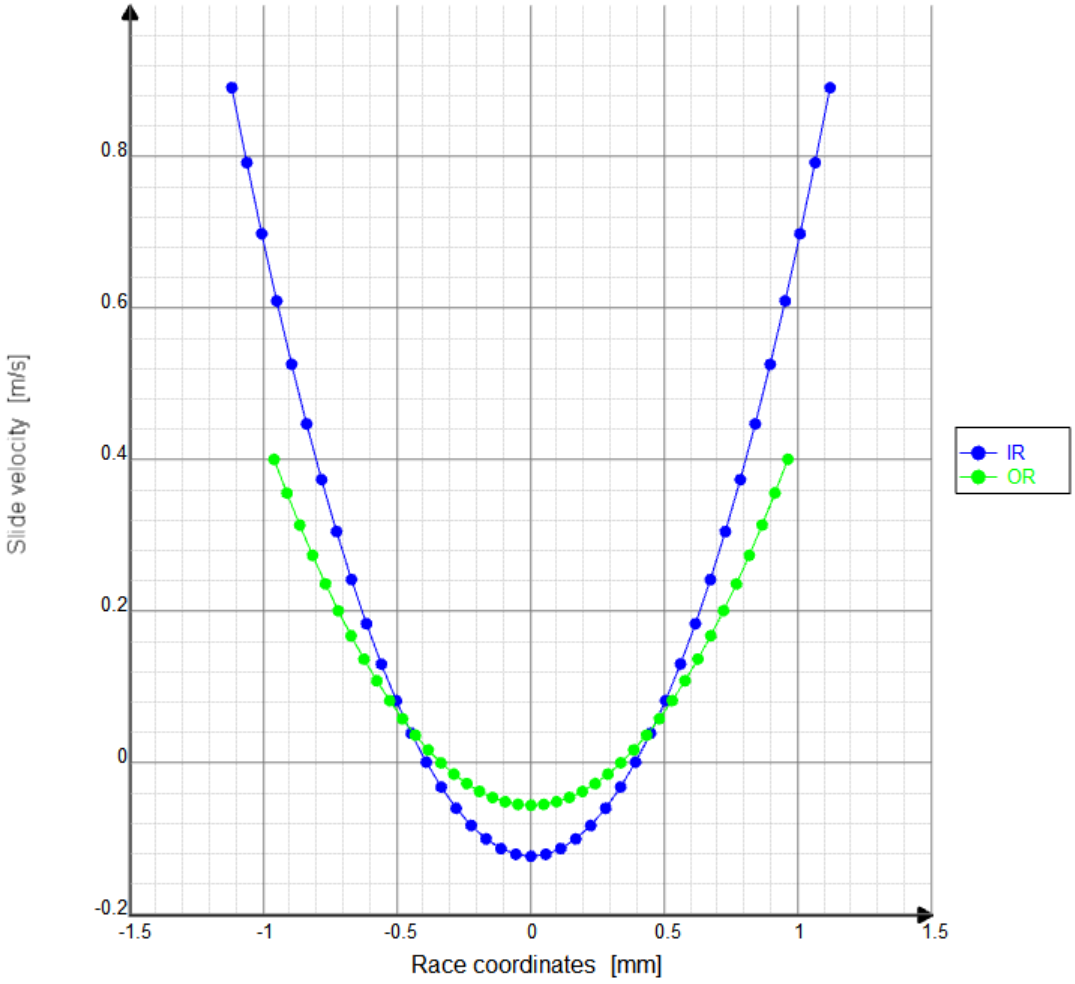

(a) Sliding Speed

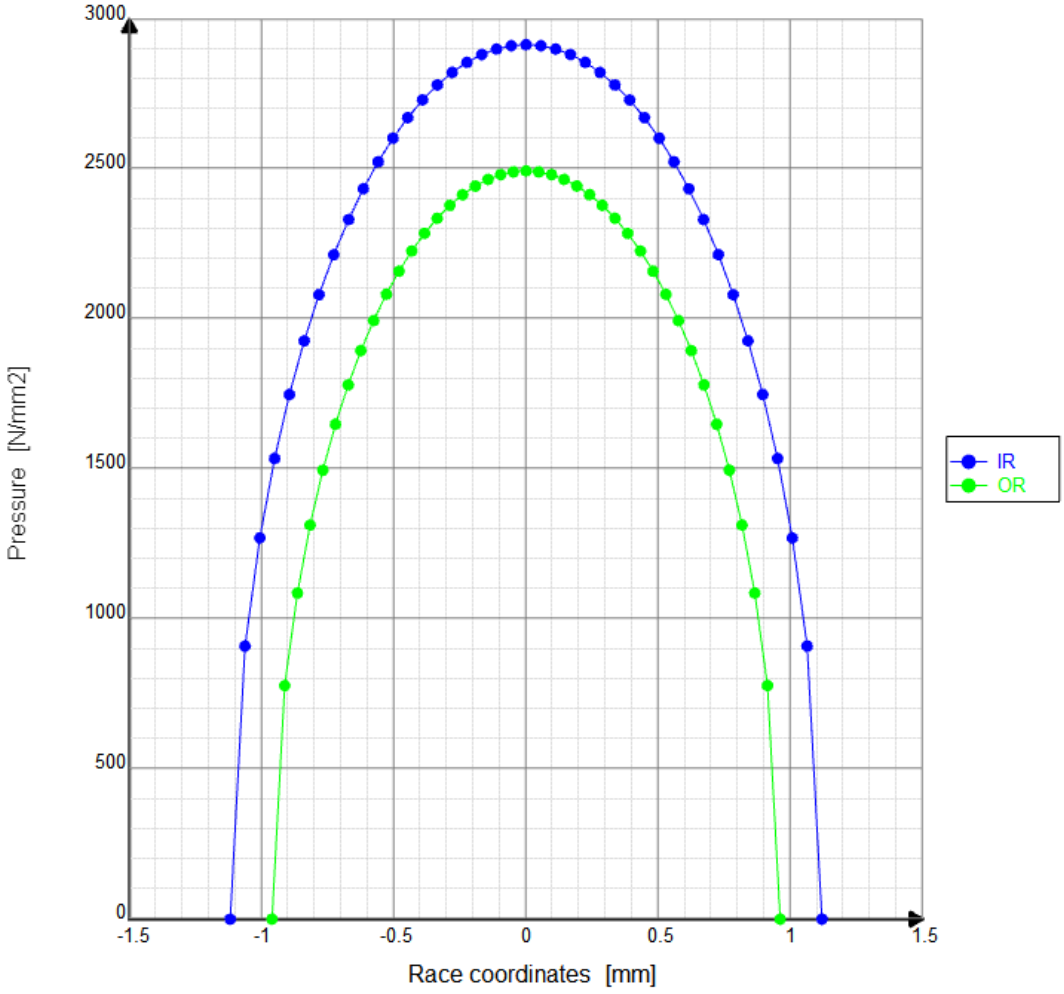

(b) Pressure distribution

Figure 3. (a) *Sliding speed distribution and (b) Contact pressure in the inner and outer ring contacts under the endurance test conditions of Table 2.*

With this information and the FFT numerical model expressed in equation (3), the temperature distribution on the contacting surfaces can be calculated. The procedure of heat partition as described in [13] is applied. Figure 4 shows the calculated raceway temperature distribution for the conditions of endurance tests of Table 2. For this calculation and the next ones a grid of $n_x = 180$ and $n_y = 170$ points has been chosen. Higher grid density does not improve the temperature calculation. The grid domain was variable to keep constant the mesh density with the values $\Delta_x = 9.0 \times 10^{-6}\ m$ and $\Delta_y = 3.55 \times 10^{-5}\ m$.

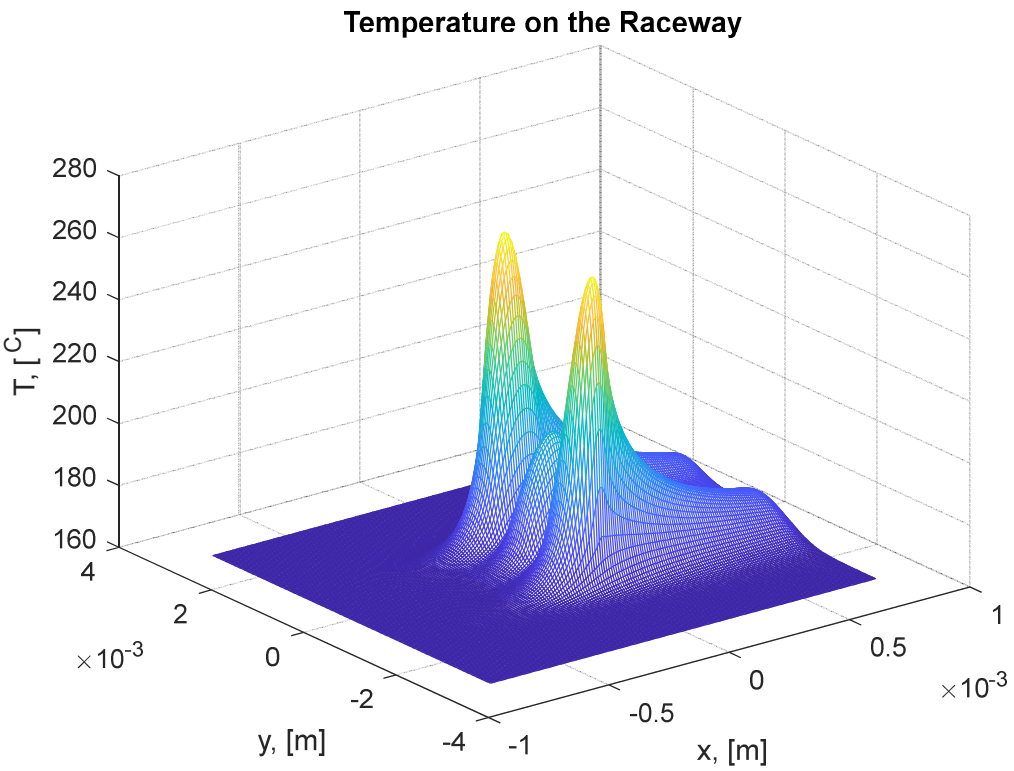

Figure 4. *Calculated temperature distribution on the inner ring raceway of for the conditions of endurance testing described in Table 2. The maximum temperature is 261⁰C.*

5.3. Surface Thermal Damage Integral

With the temperature distribution calculated above, it is now possible to calculate the surface thermal damage integral for the life equation (19).

Now, $\bar{C} = \left[\frac{(m+1)B^m}{A_D^m Ul}\right]$, in [19] for ASTM 52100 steel the values of m=11.1 and $A_D = 5979\ MPa$ are suggested, but here the value of B is to be obtained from the endurance tests. Then for the endurance test conditions of Table 2, With $l = 0.0794\ m,\ U = 11.2319\ m/s$. Therefore:

$$\frac{\bar{C}}{B^m} = 4.092 \times 10^{-108}$$

Now in these kind of bearings, softening of the hardened steel might occur only for temperatures larger than 200⁰C as recommended by the bearing manufacturer. Thus, $T_u = 200^0 C$ is selected. Besides, this bearing has 8 balls of which only three are loaded, without the constant $\bar{C}$, one can integrate the respective temperature distributions under the three different loads to obtain,

$$\sum_{i=1}^{3}\left[\int_A \langle T - T_u\rangle^m dA\right]_i = 9.4498x10^{11} + 25.18 + 25.18 = 9.4498x10^{11}$$

Only the heaviest loaded contact has an important contribution, in fact for this example the other contacts could be ignored without changing significantly the results.

Finally,

$$\underbrace{\sum_{i=1}^{N} \bar{C}^e \left[\int_A \langle T - T_u \rangle^m dA \right]_i}_{Frictional\ Heating} = 4.5223 \times 10^{-108} (B^m)^e \qquad (22)$$

From equation (22) it remains the calculation of B^m to match the experimental lives (calibration). In reality the calibration of a life model is done using many endurance tests in different conditions. In the present paper this is done only with two tests as a way to illustrate the process.

When observing the endurance tests results from the two greases one can see that if the calculation is performed only based on fatigue, i.e. the two first integrals of equation (19), no differentiation will be found in the life estimation. This is due to the fact that "*theoretically*" the two greases will produce nearly the same lubrication quality parameter κ, and in principle will also "*theoretically*" give the same kinematic starvation performance at the same speed. Thus, the differentiation must come from an external factor, e.g. bleeding rate, certain grease additives, thickener, etc. Bleeding cannot be considered here as a kinematic starvation effect modelled as in [9], because it will modify the availability of oil in the raceway in an unknown way. Protective effect of thickener or additives will also be unlikely to be modelled as fatigue. But the final effects are observed from the bearing failures in the test and they are thermal, thus they can be included in the third integral. Therefore, the constant B^m can be calculated based on these two tests by comparing the calculated life based only on fatigue (two first integrals of equation (19)) versus the experimental lives. Table 4 summarises the results.

Table 4. *Summary of calculations and experimental results (conditions of Table 2) for model calibration.*

Test	Experimental Life, L10,10, [Mrevs]	Experimental Life, L10,50, [Mrevs]	Calculated fatigue life (only two first integrals), [Mrevs]	Calibrated integral $\sum_{i=1}^{N} \bar{C}^e \left[\int_A \langle T - T_u \rangle^m dA \right]_i$	Predicted Life, all terms equation (19), [Mrevs]
Grease 1	6.049	26.11	230	4.0452×10^{-11}	59.4
Grease 2	108.91	216.51	230	1.6087×10^{-12}	204.5

From the results of Table 4 it can be seen that the predictions of the calibrated model follow the experimental trend. For the case of grease 2 the predicted life lays between the experimental percentiles L10,10 and L10,50. While for grease 1 the predicted life lays just above L10,50. In order to be conservative ideally all calculations need to be below L10,50, but for a first estimation, the results are acceptable.

5.4. High Speeds and Lower Thermal Conductivity

Once the model has been calibrated, it can be used to make predictions outside the calibration conditions. For example, in [9] several bearing tests show that there are limits to avoid seizure failures for the combination of high speeds and high loads in rolling bearings. The results for steel-steel bearings obtained in [9] are summarised in Figure 5, adapted from

Figure 7 of the reference [9]. Where, the point marked with a star ($p_h = 1.8\,GPa$ and $nd_m = 900000$) will be studied in this section using the same bearing as in Table 2. Therefore Table 5 shows now the new running conditions considered in this bearing. For comparison a high-strength bearing stainless steel with lower thermal conductivity is also used for comparison, the fatigue strength for this material is the same or higher than ASTM 52100 steel. The material properties are also included in Table 3.

Table 6 summarises the results obtained from the modelling. It must be pointed out that grease 1 was assumed with less good capability to lubricate high speed bearings, thus an average friction coefficient corresponding to boundary lubrication ($\mu = 0.16$) is assumed.

Table 5. *Summary of the new running conditions for the investigation of seizure risk.*

Bearing designation	Nominal κ	T_{bulk} [^{0}C]	Lubricant	Material	Radial Load [N]	Static p_h, inner ring, [GPa]	nd_m
6202	0.63	160	Grease 1,2	52100	300	1.8	900000

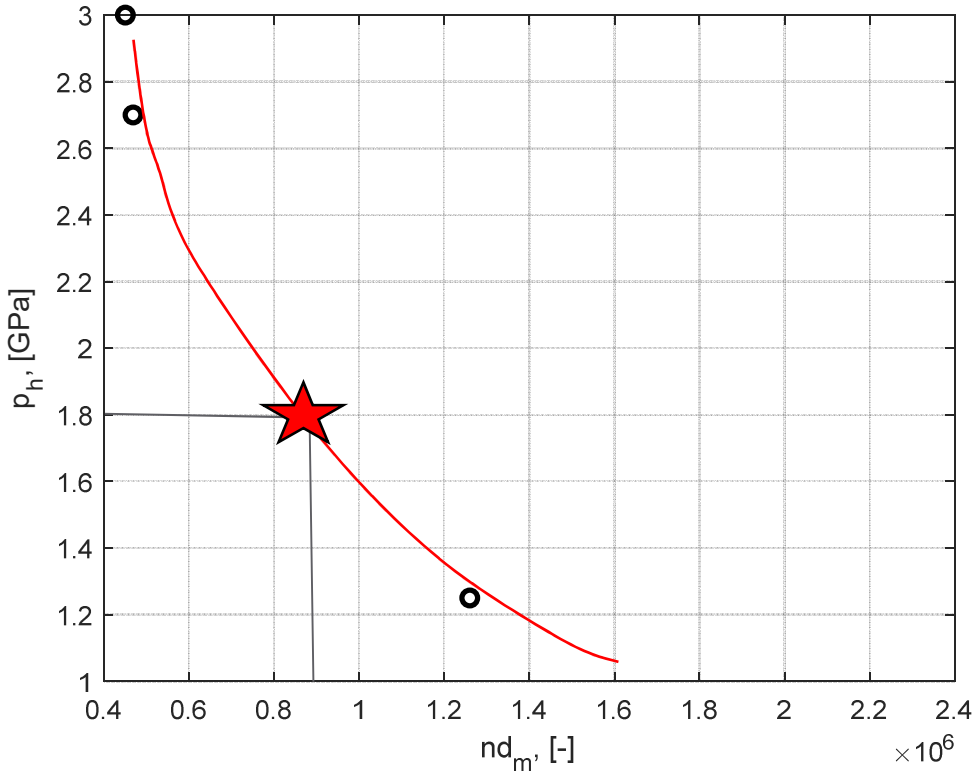

Figure 5. *Suggested limits for seizure in steel-steel rolling bearings as given in [9]. The point marked with an star is the new condition modelled in this article.*

Table 6. *Calculated lives for the star point of Figure 5.*

Nd_m	p_h [GPa]	Steel	Critical element	μ	Calibrated integral $\sum_{i=1}^{N} \bar{C}^e \left[\int_A \langle T - T_u \rangle^m dA\right]_i$	Calculated L_{10} (only fatigue) [Mrev]	Calculated L_{10} (all terms) [Mrev]

900000	1.8	52100	IR	0.16	4.48×10^{-12}	235900	539.2
900000	1.8	Stainless	IR	0.16	4.4396×10^{-11}	235900	68.5

For completeness Figure 6 shows the calculated temperatures on the raceways for the conditions given in Tables 5 and 6 for the two steels.

The results of Table 6, show an important reduction of predicted life for the steel ASTM 52100 at these new operating conditions, even when the pressure was very much reduced in comparison to the endurance testing conditions described in Table 2.

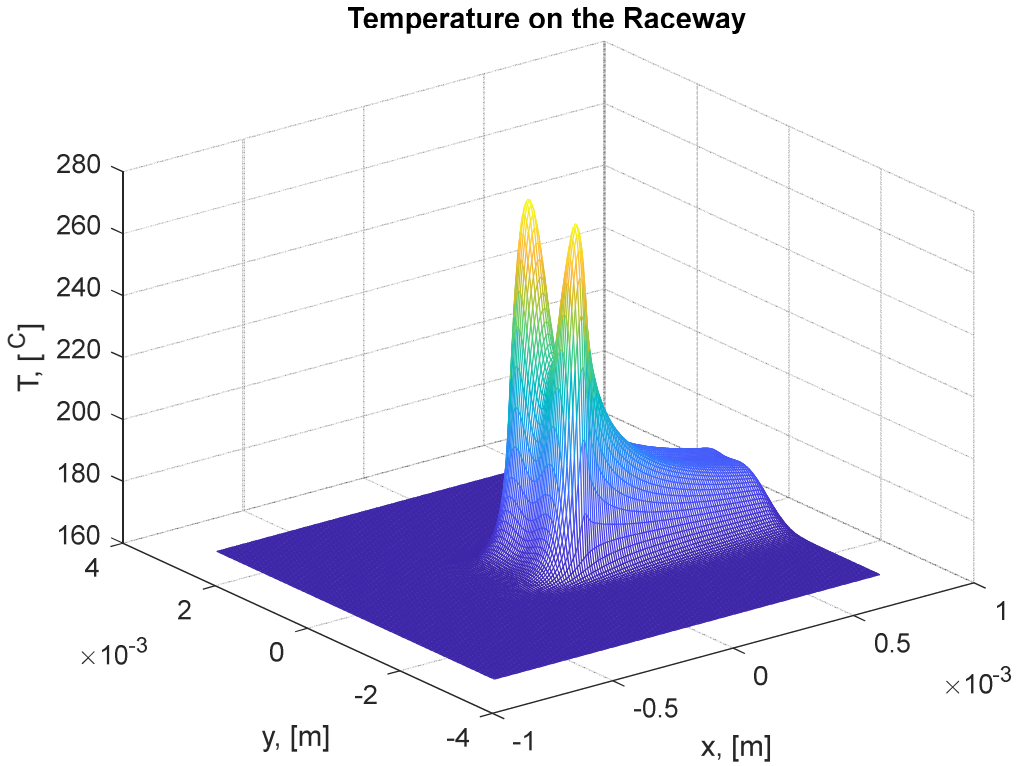

(a) – Temperature for steel ASTM 52100, $T_{max} = 269^0 C$

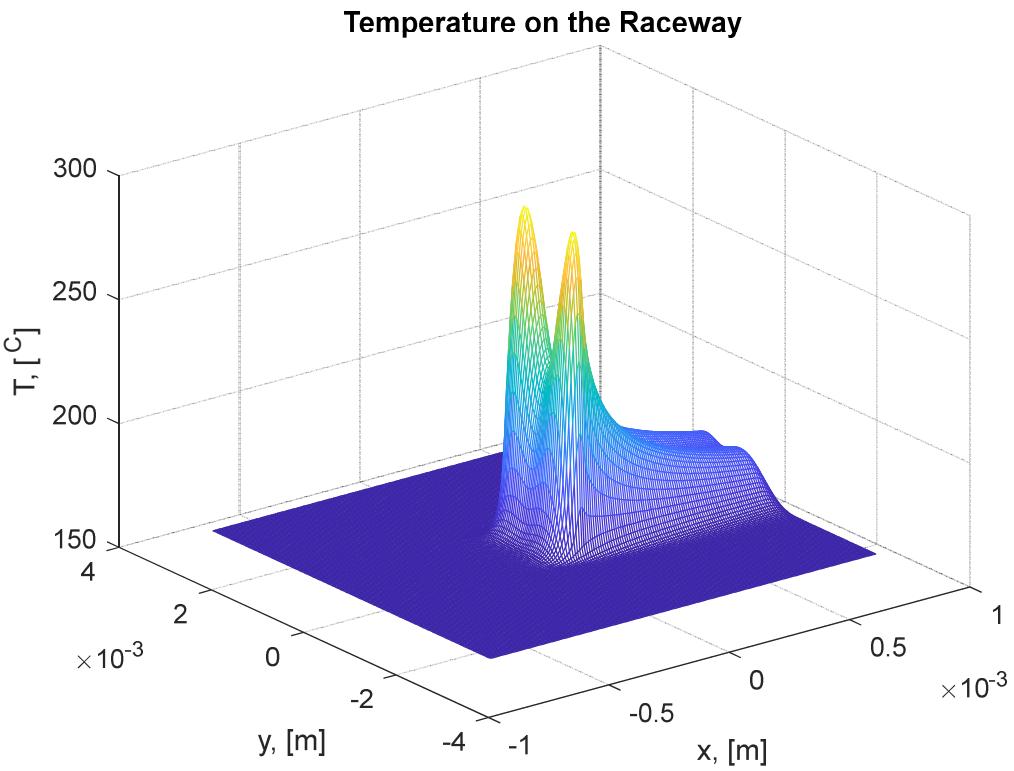

(b) – Temperature for stainless steel, $T_{max} = 286^0 C$

Figure 6. *Distribution of temperatures on the inner ring raceway for the bearing conditions described in Tables 5 and 6 with two different bearing steels.*

For the stainless bearing steel with lower thermal conductivity, Figure 6 shows higher surface temperature, which explains the even lower life calculated in Table 6 for this bearing. Clearly operating conditions close to the previously obtained seizure limit in rolling bearings [9] for standard lubrication conditions produce a much lower estimated bearing life in comparison to only fatigue mechanisms. In other words, reducing the thermal conductivity in the steel can increase the dominance of surface creep over simple fatigue (dominance of the creep integral). Pure fatigue will be controlled by the first and second integrals which do not depend on the thermal conductivity but on the endurance of the material at temperatures below T_u.

6. Discussion

A thermal damage model for tribological contacts based on creep theory is presented. The model offers the possibility to study the behaviour of failure phenomena related to surface frictional heating (i.e. smearing, scuffing, seizure) and it may also be extended to cover other failure modes in which an external heat source is at the origin of the damage (e.g. electrical current discharge damage etc.). Presently this type of surface damage is dealt by using a pass-no-pass quality criterion in which a certain threshold level of surface damage is

deemed not to be exceeded in order to maintain the reliability of the component and prevent unexpected failures.

However, it is well known that in many applications the presence of these phenomena is gradual, for relatively mild conditions. For instance, smearing in rolling bearings is often preceded by the so-called black spots (tempered material due to high temperature on the surfaces). This indicates that the damage generation is gradual and it accumulates in time, given the specific conditions. The same happens during seizure failure [9] when the conditions are mild. Here initially, raceway discolorations will appear followed by the formation of surface microcracks.

The present model provides consistent and logical results that are aligned with the observations. It has the potential to model these phenomena well showing either the gradual or sharp increase of surface damage generation as a function of the material parameters and operating conditions of the specific application case.

The thermal damage model is integrated into the generalized bearing life model [4], (that accounts for the surface and subsurface survival of the rolling contact), using an additional term representing the temperature-driven surface damage integral. As expected, this damage function follows the physics of the damage generation. Also, i) it grows when the surface temperature increases, ii) it becomes zero when the surface temperature is below the threshold limit value for creep-damage. In such a case, the service life performance of the bearing is provided, as usual, by the stress-driven high cycle fatigue of the rolling contact.

The new model when combined with a suitable rolling contact starvation model, has the potential to account for the effect of different lubrication delivery systems or mechanisms to the service life performance of the bearing. Furthermore, by including an external heat source affecting the raceway temperature, the model can in principle be adapted to account for more complex failure modes like the one occurring in case of electrical current discharge. Note that the effect of this type of failure mode on the reliability of rolling bearings is not addressed in the technical literature. Heat transfer property of the bearing material is also not considered in current life prediction models. However, using the present model, it is found that under certain operating conditions, the thermal conductivity of steel has a significant impact on the service performance of the bearing.

Note also that the use of rolling bearings under elevated thermal loads involve a number of specific application design issues, e.g. dimensional stability, hardness reduction [20], residual clearance, press fitting, thermal compatibility etc. These design issues are not included in the scope of the present paper and are not discussed. However, are significant design aspects that must be given proper consideration to enable the bearing application to reach the expected performance.

7. Conclusions

From this short investigation the following conclusions can be drawn:

1. The modified creep damage model presented in this paper has the potential to model thermally induced surface failures in tribological contacts, e.g. frictional heating, thermal distress and perhaps several others (e.g. electrical discharge damage, etc).

2. In the present model fatigue and creep are considered independent. Fatigue mainly modelled by the two initial integrals in the model while creep focused only at the surface and modelled by the third integral without inter-dependency with fatigue.

3. The present model has the ability to represent the gradual progression of thermal damage and also failure behaviours with sharp (catastrophic) characteristics. This is expected in case of tribological thermal failures which strongly depend on the thermal conditions of the rolling contact.

4. The thermal damage model is incorporated into the generalized bearing life model exploiting the modular structure of this model that allows the integration of different failure modes occurring either at the surface or in the subsurface region of the rolling contact.

5. The results obtained up to now are encouraging. The model shows consistent and logical behaviours demonstrating the advantage of the generalized bearing life in the prediction of bearing with thermally induced surface failures.

6. The ability of the generalized life model to include damaging mechanisms, other than classical metal fatigue, increases the flexibility in bearing life predictions and allows to account for phenomena previously excluded from the estimation of bearing service life.

References

1. ISO 281 (2007), “International Standard, Rolling Bearings—Dynamic Load Ratings and Rating Life,” Geneva, Switzerland.
2. Polonsky, A., Keer, L.M., “On White Etching Band Formation in Rolling Bearings,” Journal of Mechanics and Physics of Solids, Vol. 43, No. 4, pp. 637-669, 1995.
3. Zaretsky, A., STLE Life Factors for Rolling Bearings, 2nd ed., Society of Tribologists and Lubrication Engineers, Park Ridge, IL. 1999.
4. Morales-Espejel, G.E., Gabelli, A., de Vries, A.J.C., “A Model for Rolling Bearing Life with Surface and Subsurface Survival—Tribological Effects”, Trib. Trans., 58:5, pp. 894-906, 2015.
5. Morales-Espejel, G.E., Gabelli, A., “A Model for Rolling Bearing Life with Surface and Subsurface Survival: Sporadic Surface Damage from Deterministic Indentations”, Trib. Int., 96, pp. 279-288, 2016.
6. Morales-Espejel, G.E., Gabelli, A., “A Model for Gear Life with Surface and Subsurface Survival: Tribological Effects”, Wear 404–405, pp. 133–142, 2018.
7. Gabelli, A., Morales-Espejel, G.E., “A Model for Hybrid Bearing Life with Surface and Subsurface Survival”, Wear 422–423, pp. 223–234, 2019.
8. Morales-Espejel, G.E., Gabelli, A., “Application of a Rolling Bearing Life Model with Surface and Subsurface Survival to Hybrid Bearing Cases”, Proc IMechE Part C: J Mechanical Engineering Science, Vol. 233(15) pp. 5491–5498, 2019.
9. Morales-Espejel, G.E., Gabelli, A., “Rolling Bearing Seizure Effects on Fatigue Life”, Proc. IMechE, Part J: J Engineering Tribology, Vol. 233(2), pp. 339-354, 2019.

10. Carslaw, H. S. and Jaeger, J. C. “Conduction of Heat in Solids”, 2nd Edition, 1959 (Oxford Science Publications, Oxford).
11. Morales-Espejel, G.E., Wemekamp, A.W., “An Engineering Approach on Sliding Friction in Full-Film, Heavily Loaded Lubricated Contacts”, Proc. IMechE, Part J: J Engineering Tribology, Vol. 218, pp. 513-528, 2004.
12. Tian, X. and Kennedy, F. E. “Maximum and Average Flash Temperatures in Sliding Contacts”. Trans. ASME, J. Tribology,116, pp. 167–174, 1994.
13. Bos, J. and Moes, H., “Frictional Heating of Tribological Contacts”. Trans. ASME, J. Tribology, 117, pp. 171–177, 1995
14. Collins, J.A., “Failure of Materials in Mechanical Design”, Second Edition, John Wiley and Sons, New York, 1993.
15. Kachanov, L. M., 1967, The Theory of Creep, National Lending Library for Science and Technology, Boston Spa, England.
16. Rabotnov, Y. N., 1969, Creep Problems in Structural Members, North Holland, Amsterdam.
17. Lemaitre, J., Desmorat, R., “Engineering Damage Mechanics”, ISBN 3-540-21503-4 Springer Berlin Heidelberg New York. 2005.
18. Morales-Espejel, G.E., Gabelli, A., “The Behavior of Indentation Marks in Rolling–Sliding Elastohydrodynamically Lubricated Contacts”, Trib. Trans. 54 pp. 589-606, 2011.
19. Weinzapfel, N., Sadeghi, F., “Numerical Modeling of Sub-Surface Initiated Spalling in Rolling Contacts”, Tribology International 59, pp. 210–221, 2013.
20. Harris, T.A., “Rolling Bearing Analysis”, Fourth Edition, John Wiley and Sons, Inc. New York, 2001.

Acknowledgments

The authors would like to thank SKF for the permission to publish this paper.

Nomenclature

a	Hertzian semi-width, rolling direction	$[m]$
A	Contact area	$[m^2]$
$\bar{A}$	Subsurface fatigue constant	[-]
A_D	Material creep constant	$[Pa]$
$\bar{B}$	Surface fatigue constant	[-]
B	Calibration constant, representing the proportionality constant to relate surface shear stress with surface temperatures	$[Pa/K]$
C	Constant in the creep equation, $C = A_D/B$	$[Ks]$
c	Stress-Life exponent	[-]
$\bar{C}$	Constant in the thermal damage integral	$[s^{-1}m^2(Ks)^{-m}]$
d_m	Mean bearing diameter	$[m]$
D	Damage value	[-]
e	Weibull slope parameter	[-]

E	Young modulus	$[Pa]$
h	Life exponent	[-]
k_s	Thermal conductivity of steel	$[\frac{W}{mK}]$
k	Dimensional wear coefficient	$[s]$
l	Raceway length	$[m]$
p	Contact pressure	$[Pa]$
p_h	Maximum Hertzian pressure	$[Pa]$
q	Point-wise heat input per unit of area	$[\frac{W}{m^2}]$
q_0	Heat input per unit of area	$[\frac{W}{m^2}]$
R_I	Relative surface damage	[-]
R_T	Relative surface thermal damage	[-]
r_D	Material exponent in the creep equation using the nomenclature of [17].	[-]
S	Reliability	$[-]$
t	Time	$[s]$
T	Temperature	$[\,^0C]$
T_u	Limit temperature for damage	$[\,^0C]$
m	Temperature creep damage exponent	[-]
n	Bearing rotational speed	$[rpm]$
N	Number of load cycles	[-]
n_x	Number of discretization points in x	[-]
n_y	Number of discretization points in y	[-]

n_z	Number of discretization points in z	[-]
u_1	Surface speed of the rolling element	$[\frac{m}{s}]$
u_2	Surface speed of the raceway	$[\frac{m}{s}]$
U	Entrainment speed of the lubricant, $U = (u_1 + u_2)/2$	$[\frac{m}{s}]$
u	Number of load cycles per revolution	[-]
u	Surface speed	$[\frac{m}{s}]$
u_s	Sliding speed, $u_s = u_1 - u_2$	$[\frac{m}{s}]$
V_v	Integration volume, subsurface	$[m^3]$
x	Coordinate, rolling direction	$[m]$
y	Coordinate, transverse to rolling direction	[-]
z	Coordinate, normal direction to contact	[-]
ΔT	Increase in contact temperature	$[\,^0C]$
Δ_x, Δ_y	Grid distance from point to pint in x and y direction	$[m]$
v	Poisson ratio	[-]
ν	Lubricant viscosity	$[cSt]$
ρ	Density	$[kg/m^3]$
κ	Lubrication quality factor as defined in ISO 281	[-]
μ	Average Friction coefficient	[-]
σ	Stress	$[Pa]$
σ_u	Fatigue limit	$[Pa]$
χ	Thermal diffusivity, $\chi = \frac{k_s}{\rho c_p}$	$[\frac{m^2}{s}]$

Appendix A – Creep Model Solution

The solution for D in equation (11) is straightforward, first it is observed that in a tribological contact it is more convenient to count load cycles than time, therefore:

$$t = \frac{2aN}{U} \tag{A1}$$

Where t is the overall contact time of a surface, a is the Herzian semi-with in the direction of rolling, U is the speed of the surface going through the contact and N is the number of load cycles. Thus, $dt = \left(\frac{2a}{U}\right) dN$,

$$\frac{dD}{dN} = \frac{2a}{U}\left[\frac{\Delta T}{C(1-D)}\right]^m \tag{A2}$$

This equation can be re-arranged,

$$(1-D)^m \frac{dD}{dN} = \frac{2a(\Delta T)^m}{C^m U} \tag{A3}$$

Integrating equation (A3):

$$\int_0^D (1-D)^m dD = \frac{2a(\Delta T)^m}{C^m U} \int_0^N dN \tag{A4}$$

Leading to:

$$-\frac{(1-D)^{m+1}}{m+1}\Bigg|_0^D = \frac{2a(\Delta T)^m}{C^m U}\Bigg|_0^N \tag{A5}$$

From which D can be obtained:

$$D = 1 - \left[1 - \frac{2a(m+1)(\Delta T)^m N}{C^m U}\right]^{\frac{1}{m+1}} \tag{A6}$$

Or in terms of life:

$$N = \left[\frac{1}{m+1} - \frac{(1-D)^{m+1}}{m+1}\right]\frac{C^m U}{2a(\Delta T)^m} \tag{A7}$$

For which the end of the life is reached at $D = 1$, thus.

$$N_{life} = \frac{C^m U}{(m+1)2a(\Delta T)^m} \tag{A8}$$

Appendix B – Thermal Damage Model Behaviour

Figures B1 and B2 show the behaviour of equation (A6) as a function of the number of load cycles N, first for different values of m and second for different values of $\Delta T/C$. In all cases it has been assumed $\frac{2a}{U} = 0.2x10^{-3}\ [s]$. Notice that to avoid a singularity in equation (A6), a newly defined parameter K is set to:

$$for\ K > 1, take\ K = 1 \qquad (B1)$$

Where:

$$K = \frac{2a(m+1)(\Delta T)^m N}{C^m U} \qquad (B2)$$

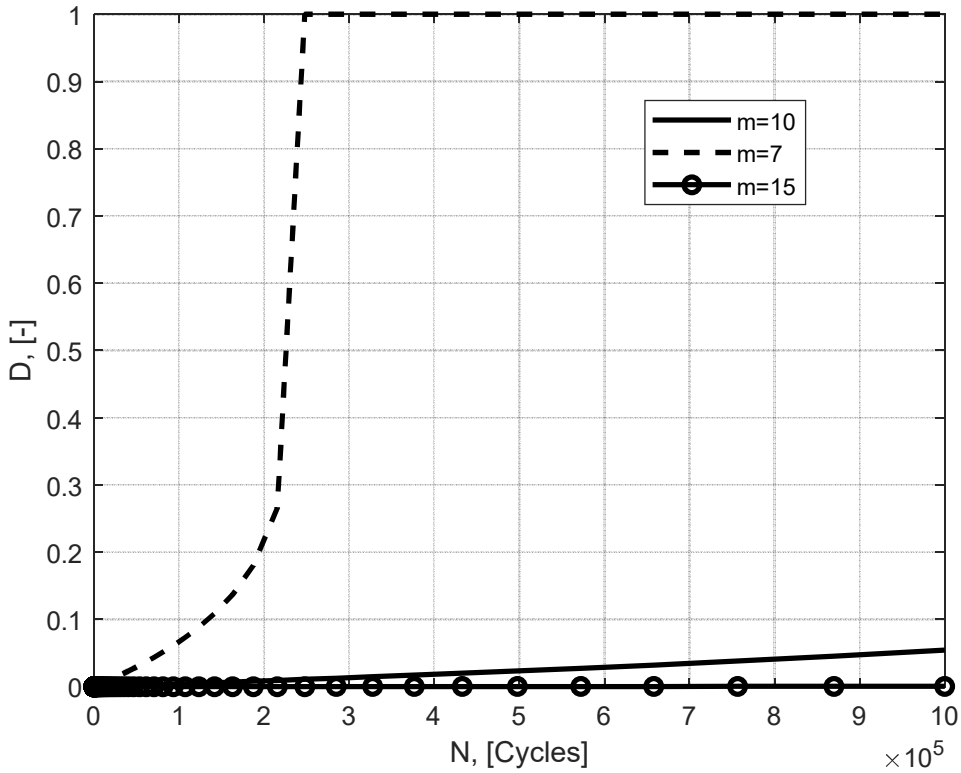

Figure B1. Equation (A6) damage parameter versus number of load cycles for different values of m and for $\frac{2a}{U} = 0.2x10^{-3}\ [s]$.

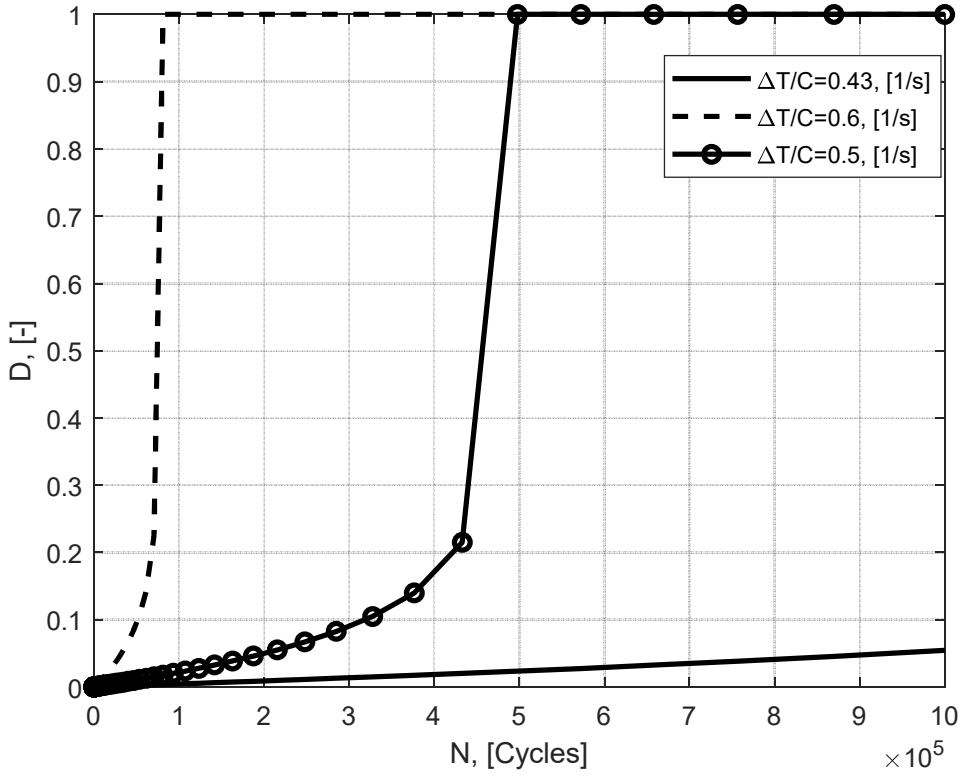

Figure B2. Equation (A6) damage parameter versus number of load cycles for different values of $\Delta T/C$ and for $\frac{2a}{U} = 0.2x10^{-3}\ [s]$.

It can be seen that increasing m has the same effect as decreasing $\Delta T/C$ or increasing C for a constant ΔT. It is also interesting to study the effect of the surface transit time in the contact. Therefore the parameter $\frac{2a}{U}$ should be varied. Figure B3 shows the results keeping constant the other two parameters. It can be seen that an slower surface (same number of load cycles) will result in more damage, which is logical, since for longer time the material is subjected to high temperatures.

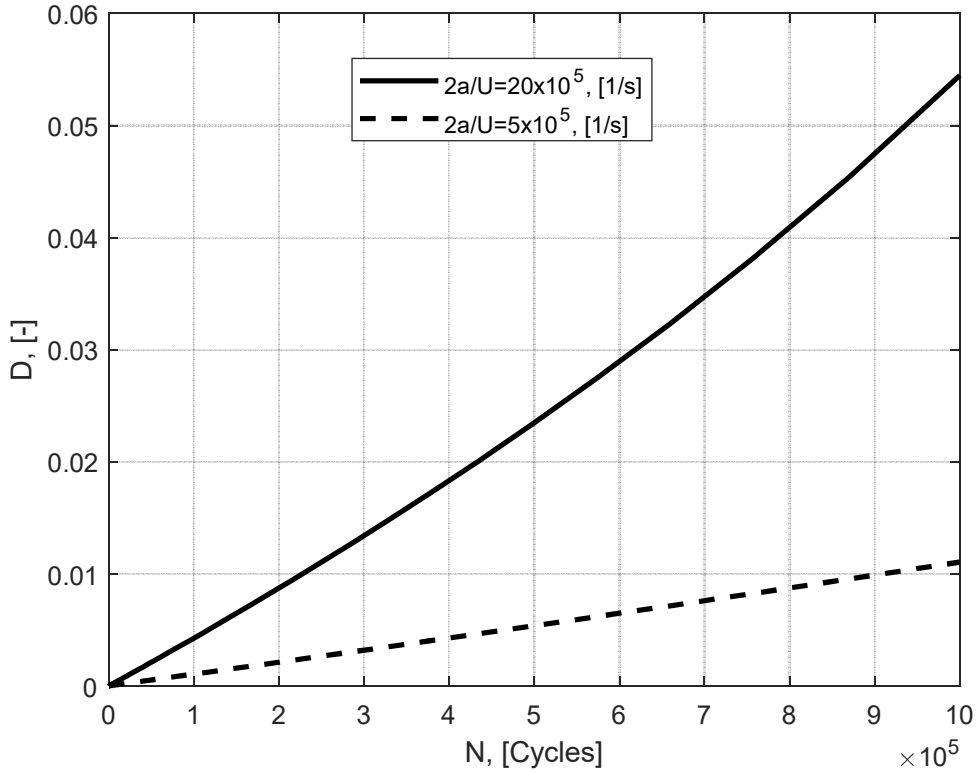

Figure B3. Equation (A6) damage parameter versus number of load cycles for different values of $\frac{2a}{U}$ and $\frac{\Delta T}{C} = 0.43$ [1/s], and $m = 10$.